*Article*

# SERS of Human Red Blood Cells in Non-Resonant Conditions: Benefits, Limitations, and Complementary Tools (CytoViva and GFAAS)

**Kelsey L. Wells [1], Praveen K. Alla [1], Kyra G. Kaiser [2], Ioana T. Murgulet [2], Norma C. Adragna [1] and Ioana E. Pavel [2,*]**

[1] Department of Chemistry and Department of Pharmacology and Toxicology, Wright State University, 3640 Colonel Glenn Hwy., Dayton, OH 45435-0001, USA; kelsey.wells@wcs.edu (K.L.W.)
[2] Department of Physical and Environmental Sciences, Texas A&M University Corpus Christi, 6300 Ocean Drive, Corpus Christi, TX 78412-5800, USA
* Correspondence: ioana.pavel@tamucc.edu; Tel.: +1-361-825-3824

Figure S1 illustrates the SERS-based sensing capabilities of the filtered, colloidal AgNPs. There is no ordinary Raman signal at an analyte (R6G test probe) concentration of $10^{-6}$ M, in the absence of AgNPs. However, a detailed, SERS spectrum with marker R6G bands could be collected within minutes after the R6G cations complexation to the negatively charged AgNPs at similar concentrations or lower.

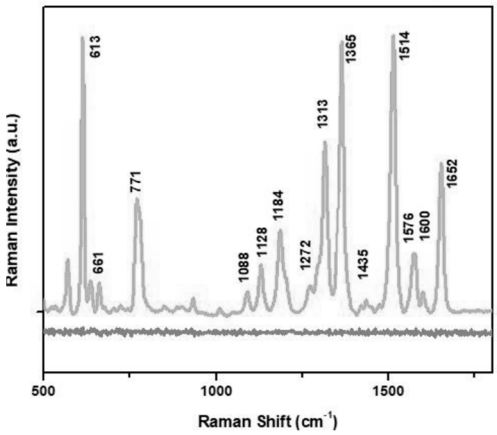


**Figure S1.** Average (n = 3) Raman control (bottom) of a $10^{-6}$ M aqueous solution of rhodamine 6G (R6G) and SERS spectrum (top) of R6G complexed at $10^{-6}$ M to filtered colloidal AgNPs in the 500–2000 $cm^{-1}$ spectral region. The spectra were manually shifted on the Y scale for comparison purposes.

Figure S2 shows the average CytoViva hyperspectra collected from n = 10 individual RBCs before (A) and after (B-D) interactions with AgNPs of different, increasing sizes, which were color coded in blue, green, and orange red. The interactions were labeled as extracellular or intracellular based on the cellular location of AgNPs at the outer membrane or cytoplasmic level, respectively.

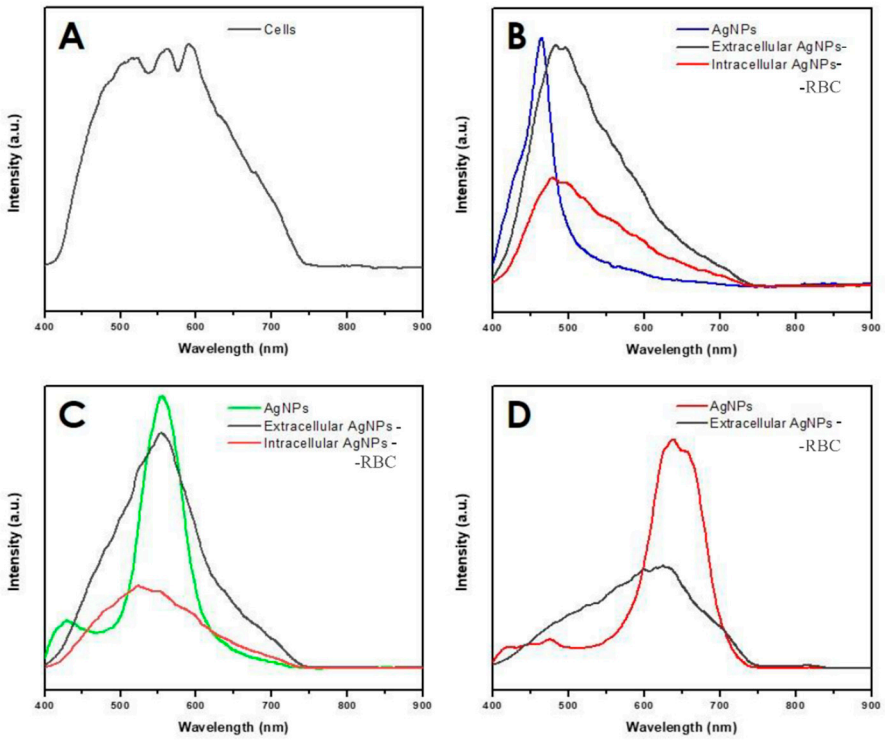


**Figure S2.** Average CytoViva hyperspectra (n = 10) of **(A)** control human red blood cells (RBCs, no AgNPs) and (b) filtered, silver nanoparticle (AgNPs) in 5% glucose medium before and after interaction with RBCs. These small AgNPs (highest spectra) were color coded in **(B)** blue, **(C)** lime green, and **(D)** orange red (before interaction with RBCs) and were denoted as extracellular or intracellular (denoted as AgNPs-RBCs after interactions with RBCs) according to their cellular locations.

Figure S3 shows the raw SERS spectrum of RBCs exposed to AgNPs (RBC-AgNPs) and the Raman control spectra of 5% glucose and 1% citrate solutions in water. These controls were utilized in the assignment of the SERS spectra collected from the RBC-AgNP samples. Negligible contributions to the marker bands of RBCs (Table S1) were noticed.

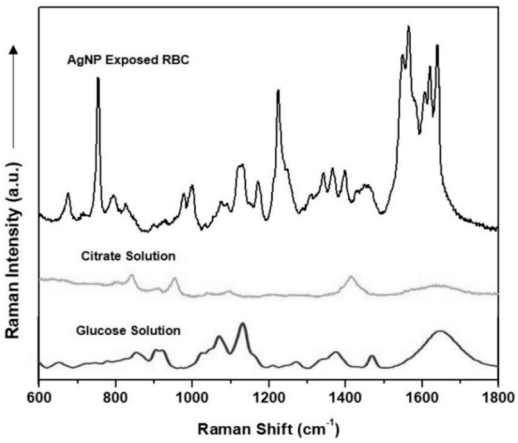


**Figure S3.** Raman spectra of 5% glucose solution, 1% citrate solution, and clustered RBCs exposed to filtered AgNPs prior to base line correction and normalization in the fingerprint region.

Figure S4 shows a typical external calibration curve for the quantification of the Ag uptake by RBCs.

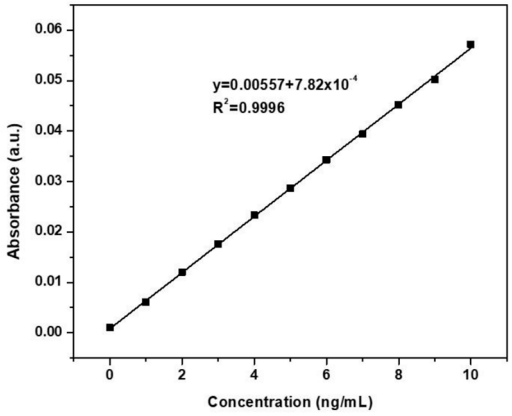


**Figure S4.** External GFAAS calibration curve constructed with n = 11 standards including one blank, in the 0–10 nm $mL^{-1}$ of Ag range. The $R^2$ value was 0.9996 for the best fit line.

Figure S5 illustrates the proposed uptake of small, citrate-capped AgNPs (< 25 nm in average diameter) through passive or facilitated diffusions across the cellular membrane of human RBCs. It should be noted that mature, normal RBCs do not exhibit receptor mediated endocytosis.

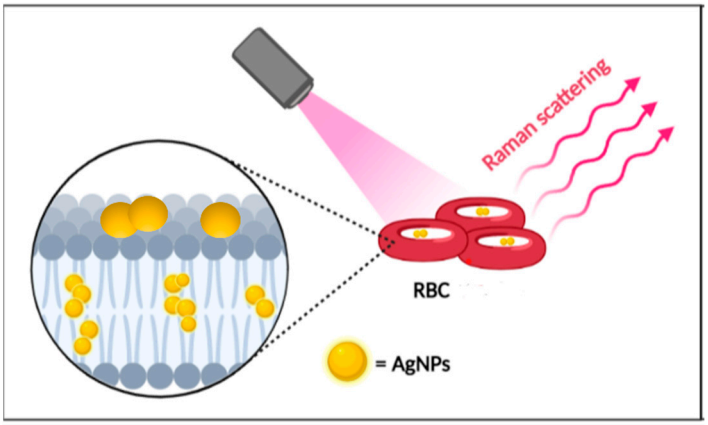


**Figure S5.** Brief schematic of the proposed passive or facilitated diffusions of small, citrate-capped AgNPs (< 10 nm in diameter) across the cellular membrane of human RBCs, while larger AgNPs (< 25 nm) are mostly interacting with the RBCs at the membrane level. Some objects might be out of scale for illustrative purposes.

Table S1 presents the tentative assignments of the Raman vibrational modes observed for the human RBCs before and after exposure to AgNPs. These bands were identified according to the literature [10-19]. **T**he spin-state 1500-1650 $cm^{-1}$ spectral region of Hb illustrates the change in the conformation of Hb from R-state (oxyHb) to T-state (deoxyHb). The ferrous, high-spin state corresponds to idealized $C_{4v}$ symmetry (Fe is ~4 nm out of the porphyrin plane). The ferric, low-spin state results in idealized $D_{4h}$ symmetry (Fe is translocated into the porphyrin plane). It should be noted that the ligation of one $O_2$ molecule pulls the $Fe^{2+}$ ion into the plane of the porphyrin ring, which facilitates the cooperative binding of other $O_2$ molecules to the three remaining heme units of Hb. Thus, the tetramer's symmetry changes upon the reversible transition from the T-state (deoxyHb) to the R-state (oxyHb).

**Table S1.** Raman vibrational modes ($cm^{-1}$) tentatively assigned according to the literature [10–19] for the human red blood cells (RBCs) before (controls) and after exposure to silver nanoparticles (individual RBC-AgNPs and irreversibly clustered RBCs-AgNPs).

| Control RBCs | Individual RBC-AgNPs | Clustered RBCs-AgNPs | Tentative Assignment |
|---|---|---|---|
| 675 | 674 | 675 | Hb: δ(pyr)<br>Proteins: ν(CS) |
| 754 | 755 | 717, 754 | Hb: δ($COO^-$)<br>Proteins: Phe and Tyr<br>Lipids: $\nu_{sym}$(C-N) of choline |
| 793 | 796 | 794 | Hb: pyr ring breathing |
| 826 | 824 | 828 | Hb: ϒ($C_mH$)<br>Proteins: Tyr<br>Lipids: $\nu_{sym}$(O-P-O) of diester |
| 900 | | 899 | Proteins: ν(C-C) |
| 919 | 921 | 927 | Proteins: ν(C-C) |
| 977 | 977 | 978 | Hb: ϒ($=C_bH_2$) |
| 999 | 996 | 1000 | Hb: $\nu_{asym}(C_\beta C_1)$ and Phe<br>Proteins: ν(C-C) |
| 1075 | 1076 | 1076 | Hb: δ($=C_bH_2$)<br>Lipids: ν(C-O) |
| | 1089 | 1091 | Hb: $\nu_{asym}(C_\beta C_1)$ or δ($=C_bH_2$) |
| 1126 | 1123 | 1122-1130 | Hb: $\nu_{asym}$(pyr half ring)<br>Proteins: ν(C-N) and ν(C-C)<br>Lipids: $\nu_{asym}(PO_2^-)$ |
| 1151 | 1150 | 1152 | Hb: $\nu_{asym}$(pyr half ring) |
| 1172 | 1172 | 1173 | Hb: $\nu_{asym}$(pyr half ring) |
| 1214–1225 | 1214–1226 | 1215–1225 | Hb: δ($C_mH$)<br>Proteins: Amide III<br>Lipids: $\nu_{asym}(PO_2^-)$ |
| 1249 | 1250 | 1249 | Hb: $\nu_{42}$<br>Proteins: Amide III or heme aggregation |
| 1309 | 1308 | 1309 | Hb: δ($C_mH$)<br>Proteins: Phe, Glu, and His ($CH_2$ wagging) |
| 1342 | 1342 | 1342 | Hb: $\nu_{sym}$(pyr half ring)<br>Proteins: Glu, Asp, and Gln ($CH_2$ scissoring) |
| 1367 | 1367 | 1367 | Hb: $\nu_{sym}$(pyr half ring) |
| 1398 | 1398 | 1399 | Hb: $\nu_{sym}$ (pyr quarter-ring) |
| 1428 | 1428 | 1430 | Hb: $\nu_{sym}(C_aC_m)$<br>Protein: Tyr |
| | 1452 | | Hb and Lipids: δ($CH_2$/$CH_3$) |
| 1460 | | 1460 | Hb: $\nu_{sym}(C_aC_m)$ and δ($CH_2$) |
| 1549 | 1547 | 1550 | Hb: $\nu(C_\beta C_\beta)$ |
| 1566 | 1567 | 1566 | Hb: $\nu(C_\beta C_\beta)$ |
| 1580 | 1576 | 1583 | Hb: $\nu_{asym}(C_aC_m)$ |
| 1609 | 1609 | 1607 | Hb: $\nu(C_a{=}C_m)$ |
| 1620 | - | 1620 | Hb: $\nu(C_a{=}C_b)$ |
| 1640 | 1639 | 1640 | Hb: $\nu_{asym}(C_aC_m)$<br>Proteins: amide I |

**Abbreviations**: sym - symmetric, asym - asymmetric, ν - stretching, δ - in plane deformation, ϒ - out of plane deformation, pyr - pyrrole, Phe - phenylalanine, Tyr - tyrosine, Glu – glutamic acid, Asp – aspartic acid, Gln - glutamine, His - histidine, and m – methine.

Table S2. summarizes the position, integrated area, and full-width-at-half-maximum (FWHM) values for the discussed marker peaks in the 1500–1650 $cm^{-1}$ spectral region.

**Table S2.** Position, integrated area, and full-width-at-half-maximum (FWHM) values for the discussed marker peaks in the 1500–1650 $cm^{-1}$ spectral region.

| | Integrated areas | | |
|---|---|---|---|
| **Peak position ($cm^{-1}$)** | **Control RBCs** | **Individual RBC-AgNPs** | **Clustered RBCs-AgNPs** |
| 1609 | 16.8±3 | 23.3±1 | 15.9±7 |
| 1620 | 2.4±1 | - | 7.3±3 |
| 1640 | 18.4±1 | 9.6±2 | 22.7±0.8 |
| | | FWHM ($cm^{-1}$) | |
| 1609 | 20.5±1 | 25.5±1 | 22.2±1 |
| 1620 | 8.3±1 | - | 11.1±1 |
| 1640 | 32.7±1 | 36.1±1 | 21.6±1 |

Table S3 summarizes the *t*-values with 95% confidence intervals for the three post-washes with glucose of human RBCs. The release of hemoglobin into the supernatant was not significant during the third wash. This means that two washes sufficed in the removal of most lysed cells and cellular debris. However, three pre-washes were performed in all experiments to ensure full restoration of membrane function and shape and is in good agreement with the RBC literature.

**Table S3.** Results of the statistical *t*-test showing the efficiency of five subsequent washes of human RBCs with glucose. They were established with respect to the differences in the absorbance maxima of the most intense band, *i.e.*, the Soret band at 417 nm.

| **Washes** | **Experimental *t*-value** | **Significance** |
|---|---|---|
| 1–2 | 3.48 | Significant |
| 2–3 | 2.22 | Not significant |
| 3–4 | 1.33 | Not significant |
| 4–5 | -1.52 | Not significant |